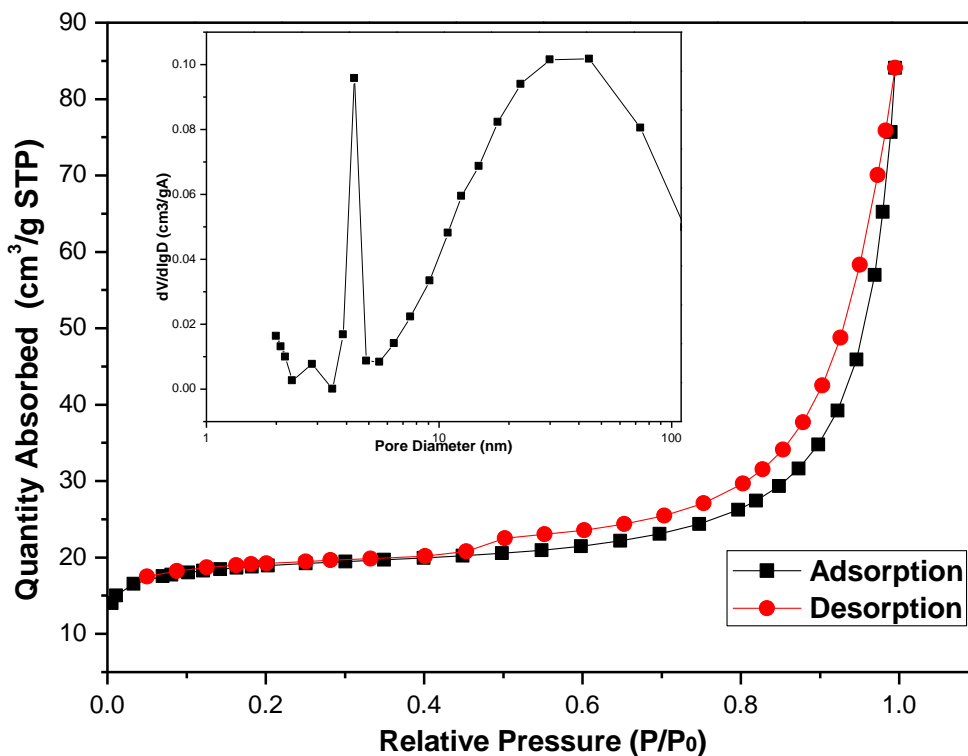


## Supporting Information

### MnO@1-D carbon composites from the precursor of $C_4H_4MnO_6$ and their high-performance in lithium batteries

Xiaona Li,<sup>a</sup> Yongchun Zhu,<sup>\*a</sup> Xing Zhang,<sup>a</sup> Jianwen Liang,<sup>a</sup> and Yitai Qian<sup>\*a,b</sup>

#### 1. $N_2$ adsorption/desorption measurements of the MnO@1-D carbon composites.



**Fig. S1 Nitrogen adsorption-desorption isotherm and the corresponding pore size distribution (inset) of the MnO@1-D carbon composites.**

The MnO@1-D carbon composites have a Brunauer–Emmett–Teller (BET) surface area of  $64 \text{ m}^2 \text{ g}^{-1}$ , and the average pore size is at ca. 24.57 nm. It is noticeable that the materials are mainly composed of microporous and mesoporous structure. The high specific surface area and the porous nature of the MnO@1-D carbon composites are very favorable to lithium ion and electron transport.

#### 2. XRD patterns of the products under different annealing temperatures and times.

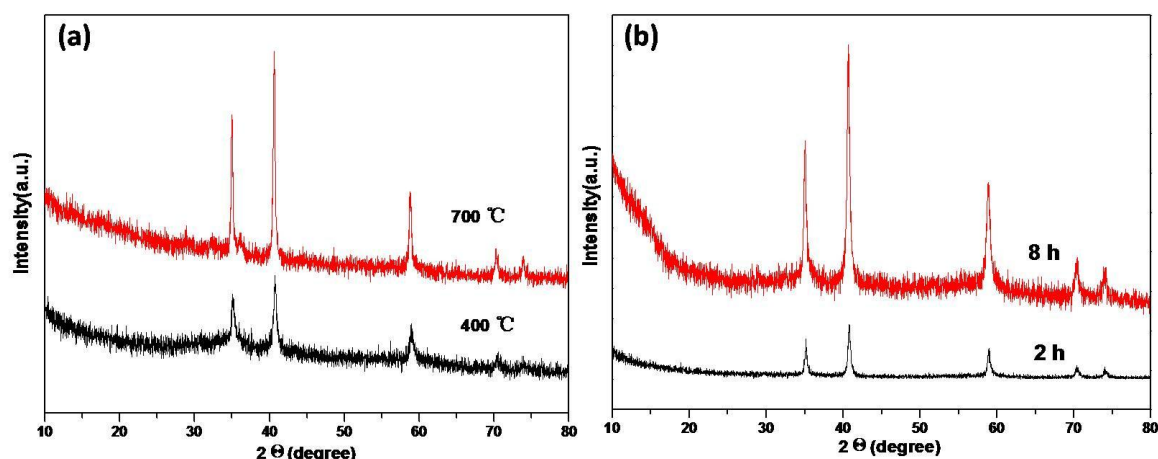


**Fig. S2 (a)** XRD patterns of the products annealing at 400 °C and 700 °C for 4h, respectively, **(b)** XRD patterns of the products annealing at 500 °C for 2h and 8h, respectively

### 3. SEM images of the products under different annealing temperatures and times.

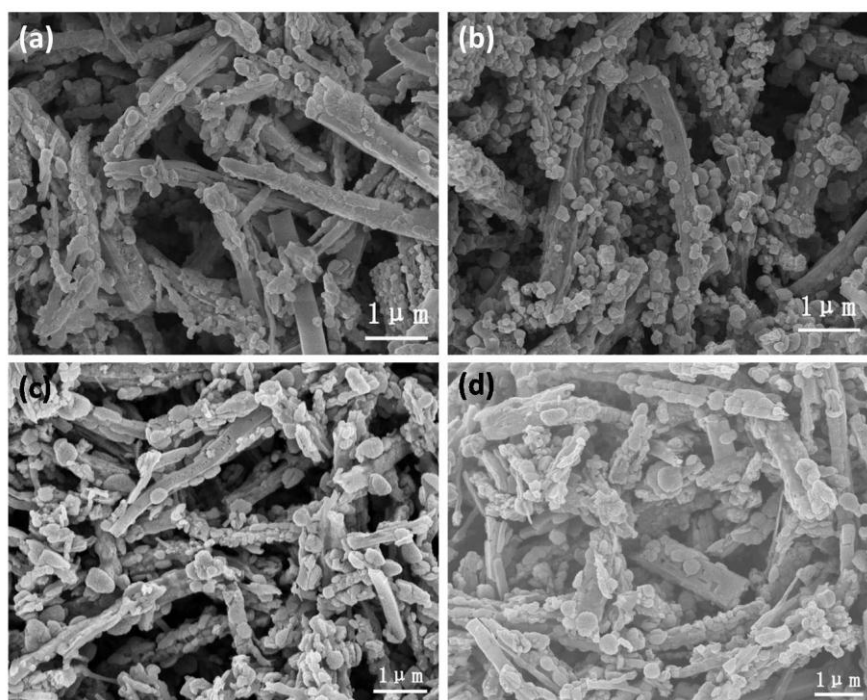


**Fig. S3 SEM images of the products under different temperatures.**(a) (b) annealing at 400 °C and 700 °C for 4h, respectively, (c) (d) annealing at 500 °C for 2h and 8h, respectively.

The dispersion state of MnO nanoparticles was found to strongly depend on the annealing temperature. When annealed at 400 °C or 700 °C, MnO@1-D carbon composites can also be obtained (Fig. S3). As the annealing temperature increasing from 400 to 700 °C, more MnO nanoparticles are adherent to the surface of the 1-D carbon skeleton rather than those wrapped inside. And those MnO nanoparticles are agglomerated together instead of dispersed well in the 1-D carbon skeleton when annealed under higher temperature. While annealed at 500 °C for 2h or 8h, the dispersion of MnO nanoparticles is almost the same.

#### 4. Cycle performance of the MnO@1-D carbon composites obtained under different annealing temperatures and times.

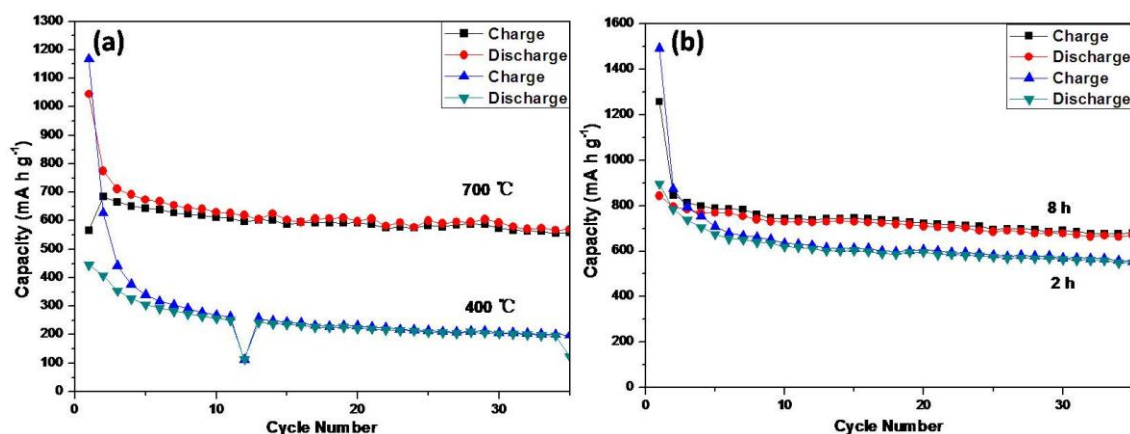


**Fig. S4** Cycle performance of the MnO@1-D carbon composites.(a) annealing at 400 °C and 700 °C for 4h, respectively, (b) annealing at 500 °C for 2h and 8h, respectively. (Current rate of 100 mA g<sup>-1</sup>)

In contrast, other MnO@1-D carbon composites obtained at different conditions were also employed as anode materials. Apparently, all of the capacities of the samples obtained under different annealing temperatures and times are lower and drop faster than those of the samples obtained at 500 °C for 4h(Fig. S4). Thus, there may be a close correlation between the electrochemical performance and the combining ways in the MnO@1-D carbon composites, which include good spatial distribution of MnO nanoparticles in 1-D carbon skeleton and appropriate proportion of those MnO nanoparticles wrapped inside or adherent to the surface of the 1-D carbon skeleton. For the samples with more MnO nanoparticles wrapped inside, the formed SEI film and the carbon skeleton decrease the electrical contact of the active MnO nanoparticles. On the other hand, for the samples with more MnO nanoparticles adherent to the surface of the 1-D carbon skeleton, the size of the of the active MnO nanoparticles are bigger, which is not good for the transformation of Li<sup>+</sup>, and most of the active nanoparticles are in the surface of the carbon skeleton, the whole carbon

network cannot prevent the agglomeration and the pulverization of the active nanoparticles.

**5. Cycle performance of the MnO@1-D carbon composites with lower conductive carbon (20% conductive carbon with 70% active material and 10% binder).**

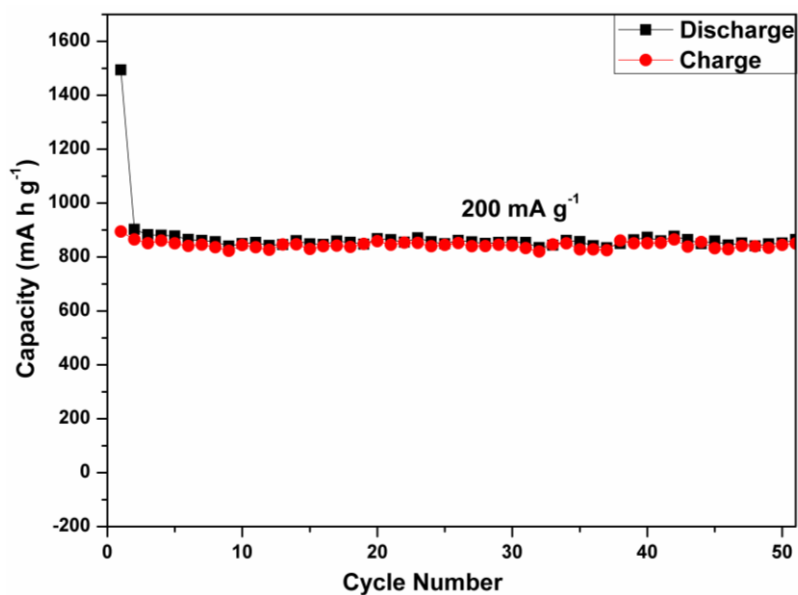


**Fig. S5 Cycle performance of the MnO@1-D carbon composites with lower conductive carbon. (Current rate of 200 mA g<sup>-1</sup>)**